Letters 13, 643 (1964); J. M. Charap and P. T. Matthews, Phys. Letters 13, 346 (1964); T. K. Kuo and T. Yao, Phys. Rev. Letters 14, 79 (1965); K. J. Barnes, P. Carruthers, and Frank von Hippel, Phys. Rev. Letters 14, 82 (1965).

[2]R. P. Feynman, M. Gell-Mann, and G. Zweig, Phys. Rev. Letters 13, 678 (1964). K. Bardakci, J. M. Cornwall, P. G. O. Freund, and B. W. Lee, Phys. Rev. Letters 13, 698 (1964); 14, 48 (1965). S. Okubo and R. E. Marshak, Phys. Rev. Letters 13, 818 (1964); W. Rühl, Phys. Letters 13, 349 (1964); A. Salam, Phys. Letters 13, 354 (1964); T. Fulton and J. Wess, Phys. Letters 14, 57 (1965); P. Roman and J. J. Aghassi, Phys. Letters 14, 68 (1965); M. A. B. Bég and A. Pais, Phys. Rev. (to be published).

[3]G must contain SL(6,c) as a subgroup. See L. Michel and B. Sakita, to be published.

[4]S. Coleman, private communication.

[5]This assumption is consistent with the model in which every particle is constructed from one or more of the fundamental triplets.

[6]Invariance under SL(6,c) and space reflections permits also the interactions of the type $g\,\mathrm{Tr}(\Phi\gamma_5\Phi\gamma_5\Phi)$. L_{int} in Eq. (4) is invariant under a larger group $M(12)$ [or $\tilde{U}(12)$]: K. Bardakci, J. M. Cornwall, P. G. O. Freund, and B. W. Lee, Phys. Rev. Letters 14, 48 (1965); R. Delbourgo, A. Salam, and J. Strathdee, to be published.

[7]R. J. Duffin, Phys. Rev. 54, 1114 (1938); N. Kemmer, Proc. Roy. Soc. (London) A173, 91 (1939). The use of the Duffin-Kemmer equation in SU(6) theory was suggested to us by Professor L. A. Radicati.

[8]We would like to note here that Eq. (5) can be derived from the free Lagrangian $-\frac{1}{2}m\Phi_A{}^{i\alpha}(\gamma\cdot\partial+m)_i{}^j\times\Phi_{j\alpha}{}^A$. However, we do not know of any simple free Lagrangian from which Eq. (9) can be derived. The quantization of Ψ field needs further investigation.

[9]W. Rarita and J. Schwinger, Phys. Rev. 60, 61 (1941).

[10]Decuplet part of Eq. (9) is the Bargmann-Wigner equation for a spin-$\frac{3}{2}$ particle. V. Bargmann and E. P. Wigner, Proc. Natl. Acad. Sci. U. S. 34, 211 (1948).

[11]Following Bég and Pais, we take $M=1065$ MeV, $m=615$ MeV. See reference 2.

[12]The use of lowest order perturbation theory is unreasonable from the point of view of strong-interaction theory. Our results, however, can be obtained assuming that the vertex functions are invariant under $M(12)$.

[13]The rectangular bracket in Eq. (13) implies taking the trace with respect to SU(3) indices.

[14]M. Gell-Mann, D. Sharp, and W. G. Wagner, Phys. Rev. Letters 8, 261 (1962).

[15]$J_A{}^B(\bar{B}D)=[J_B{}^A(\bar{D}B)]^\dagger$.

[16]The SU(3) decomposition and the corresponding expressions for these currents in the nonrelativistic SU(6) theory are to be found in B. Sakita, Phys. Rev. Letters 13, 643 (1964).

[17]F. J. Ernst, R. G. Sachs, and K. C. Wali, Phys. Rev. 119, 1105 (1960).

[18]R. G. Sachs, Phys. Rev. 126, 2256 (1962); Phys. Rev. Letters 12, 231 (1964).

[19]A. Salam, Proceedings of the Second Coral Gables Conference on Symmetry Principles at High Energies, University of Miami, January 1965 (to be published).

$\pi^- + p \to \pi^0 + n$ CHARGE-EXCHANGE SCATTERING AT HIGH ENERGIES*

I. Mannelli,† A. Bigi, and R. Carrara
Istituto di Fisica dell' Università, Pisa, Italy,
and Istituto Nazionale di Fisica Nucleare, Sezione di Pisa, Pisa, Italy

and

M. Wahlig and L. Sodickson‡
Laboratory for Nuclear Science, Massachusetts Institute of Technology, Cambridge, Massachusetts

(Received 27 January 1965)

We report here the differential and total cross sections for elastic charge-exchange scattering $\pi^- + p \to \pi^0 + n$ at incident lab pion momenta of 6, 8, 10, 12, 14, 16, and 18 GeV/c.[1] Measurements were made at values of the four-momentum transfer squared between 0 and −0.5 (GeV/c)^2. This represents the high-energy part of a recent spark-chamber run at the Brookhaven AGS; preliminary results of the lower energy part of this run (2.4 to 6 GeV/c) have been published previously.[2]

Only minor changes were made to the experimental apparatus as described in reference 2. The length of the liquid-hydrogen target was increased from 2 to 6 in., and the distance between it and the spark chamber was increased with increasing energy. The spark chamber was triggered each time a π^- entered the target and failed to produce an "anti" signal in any of the surrounding scintillation counters. For all of the data reported here, the counters at the rear of the spark chamber (which in reference 2 served to confirm the presence of a shower in the spark chamber) were not used.

The beam used for the 6- through 18-GeV/c run was the one originally set up by Galbraith

et al.,[3,4] and it included a differential Cherenkov counter to discriminate against K^- and $\bar{p}$. The momentum spread was ±2% at half-height of a triangular distribution, and the angular divergence was smaller than 2 mrad.

All the pictures have been scanned twice for two-shower events. Showers were accepted only if they originated within a fiducial volume and had a minimum of four sparks per track. With this condition the conversion probability for a high-energy γ ray incident normal to the spark chamber was about 95%.

The raw data have been corrected for the following:

(1) The empty-target counting rate. This is subtracted after normalizing to the same number of effective incident π^- obtained for the corresponding full-target run. It amounts typically to a 10% effect.

(2) The probability that one or both γ rays convert before reaching the fiducial volume of the spark chamber (~9%). The probability that one or both γ rays pass through the fiducial volume without converting in it is included in the Monte-Carlo efficiency calculation described below.

(3) The μ^- contamination of the beam (4.7 ± 1%).

(4) The fraction of events missed in scanning. By comparison of two independent scannings of all the pictures, the scanning efficiency has been estimated to be 98 ± 2%.

(5) The beam attenuation in the hydrogen target. With the 6-in. target, this is a 0.9% effect.

(6) The Dalitz-pair decay mode (~1%).

(7) The probability that the recoil neutron gives a signal in the "anti" counters (typically 1%).

No correction has been applied for the electron contamination of the beam, nor for possible triggering or spark-chamber inefficiencies, all of which are small compared to the corrections described above.

The opening angle between the two γ rays, $\theta_{\gamma\gamma}$ (all angles here are in the $\pi^- p$ c.m. system), is obtained from the measured position of the first spark in each shower, under the assumption that the event originated at the center of the hydrogen target. The largest source of error in $\theta_{\gamma\gamma}$ is due to the length of the hydrogen target relative to the distance between the hydrogen target and spark chamber. This uncertainty in $\theta_{\gamma\gamma}$ varied between ±1.6 and ±2.5% for the various spark-chamber positions.

The distribution of $\theta_{\gamma\gamma}/\theta_{\gamma\gamma\,\mathrm{min}}$ (which ratio we will denote as $R_{\mathrm{c.m.}}$), where $\theta_{\gamma\gamma\,\mathrm{min}}$ is the minimum value of $\theta_{\gamma\gamma}$ for an elastic charge exchange π^0, peaks sharply at $R_{\mathrm{c.m.}} = 1.0$. We insure a predominantly elastic sample of events by limiting our data to events whose $R_{\mathrm{c.m.}}$ values are close to 1.0; in fact we use the interval $0.965 \leq R_{\mathrm{c.m.}} \leq 1.165$, which should include about half of the elastic events. To determine more precisely what fraction, f, of the elastic events are included within this $R_{\mathrm{c.m.}}$ cut, we have made a Monte-Carlo calculation to predict the expected $R_{\mathrm{c.m.}}$ distribution, including the effects of the momentum, spatial, and angular spread of the beam, the length of the hydrogen target, and the size of the spark chamber. The agreement of this calculated distribution with the experimental distribution, as shown in Fig. 1, is good enough to determine f to better than 0.01.

This same Monte-Carlo calculation predicted the values of the angular distribution for the bisector of the γ rays that would be observed if the π^0-production angular distribution is isotropic. These values can be considered as efficiency factors in going back from the observed distribution of the bisectors to the expected π^0 differential cross section. Theoretically, this is true only when the differential cross section is a linear function of t, where t is the square of the four-momentum transfer to the nucleon. But in practice, for our cut in $R_{\mathrm{c.m.}}$ ($0.965 \leq R_{\mathrm{c.m.}} \leq 1.165$), we obtain essentially the same efficiency factors using an assumed π^0 distribution which is a good approximation to our experimental results, namely, $d\sigma/dt = \mathrm{const}$ for $0 \geq t \geq -0.1$ and $d\sigma/dt \propto e^{7.6t}$ for $t < -0.1$ (GeV/c)^2.

From the agreement between the Monte-Carlo and the experimental distribution in $R_{\mathrm{c.m.}}$ it can be safely concluded that, inside the $R_{\mathrm{c.m.}}$ acceptance region, the contamination from events with the two showers coming from two different π^0's is negligible.

The type of processes which could nevertheless seriously contaminate our sample would be abundant peripheral production of nucleon isobars $\pi^- + p \to N^{*0} + \pi^0$, where $N^{*0} \to n + \pi^0$, with the fairly low-energy γ rays from the isobars failing to trigger the anticoincidence system. We have estimated an upper limit for this contamination by using the measured isobar pro-

duction cross section, and calculating what fraction of the isobar events would fail to trigger our "anti" system when the fast π^0 satisfies our elastic acceptance criteria. Using the Lindenbaum-Sternheimer isobar model,[5] we calculated the energy spectrum of the π^0's from the isobar decay. This spectrum is only slightly sensitive to the shape of the angular distribution of the isobar production, whereas it shows a strong dependence on the isobar mass. Folding in the calculated efficiency, as a function of the energy, for the detection of γ rays in the "anti" counters, we estimate that about 10% of the events $\pi^- + p \rightarrow N^{*0} + \pi^0$, with $N^{*0} \rightarrow n + \pi^0$, produced with $0 \geq t \geq -0.5$ (GeV/c)^2 for the $N^{*0}(1238)$, would have been included in the elastic charge-exchange sample. Assuming that the peripheral isobar production is dominated by $T = 1$ exchange,[13] charge independence predicts that

$$\frac{\pi^+ + p \rightarrow \pi^0 + N^{*++}}{\pi^- + p \rightarrow \pi^0 + N^{*0}} = 3.$$

Using as a reasonable upper limit at our energies the cross section for $N^{*++}(1238)$ production measured at 8 GeV/c,[6] we calculate that this inelastic contamination is less than 10 to 20% at all our energies.

Experimentally, we can check this calculation by trying to detect the presence of such a contamination in our $R_{c.m.}$ distributions. Accordingly, we have made a detailed χ^2 comparison between our experimental $R_{c.m.}$ distributions and those predicted by a Monte-Carlo calculation for various amounts of $N^{*0}(1238)$ isobar contamination, assuming that the extra π^0 would not be detected in our "anti" system. Figure 1 shows, in addition to the experimental $R_{c.m.}$ distribution at 10 GeV/c, the Monte-Carlo predictions for 0% and 100% isobar contamination, using the Lindenbaum-Sternheimer model for the isobar mass spectrum.[5] The distance between the pure elastic and the pure isobar peaks decreases with momentum as $1/p_{\pi^-}$ where p_{π^-} is the incident pion momentum in the lab system. Contaminations from higher mass isobars would be immediately evident in the $R_{c.m.}$ distribution since they would produce a secondary peak well distinguishable from the elastic peak. The results of these $R_{c.m.}$ comparisons are consistent with zero contamination and set a maximum of 10%.

Since both our calculated and experimental estimates of the inelastic contamination yield a small percentage upper limit, we will assume that this contamination is negligible in our data.

The differential cross sections at 6, 8, 10, 12, 14, and 16 GeV/c are shown in Fig. 2 and include only the statistical errors. The overall systematic uncertainty is estimated to be ±8%; the largest contributions come from the uncertainty in the number of protons/cm^2 in the hydrogen target [estimated to be $(7.1 \pm 0.3) \times 10^{23}$], the scanning efficiency, and the μ^- beam contamination.

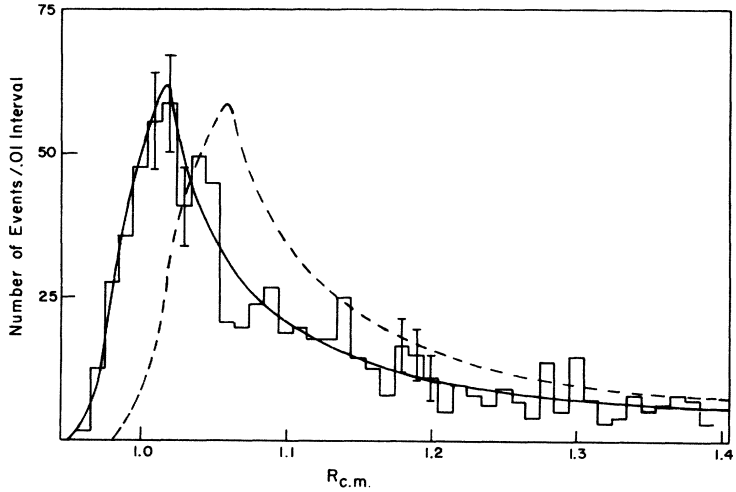

FIG. 1. The experimental distribution in $R_{c.m.}$ (histogram) at 10 GeV/c, compared with the Monte-Carlo calculation predictions for pure elastic (solid line) and pure $N^{*0}(1238)$ isobar (dotted line) charge-exchange production. The Monte-Carlo calculation curves have been normalized to the same number of events as the experimental histogram within our accepted $R_{c.m.}$ limits of 0.965 to 1.165.

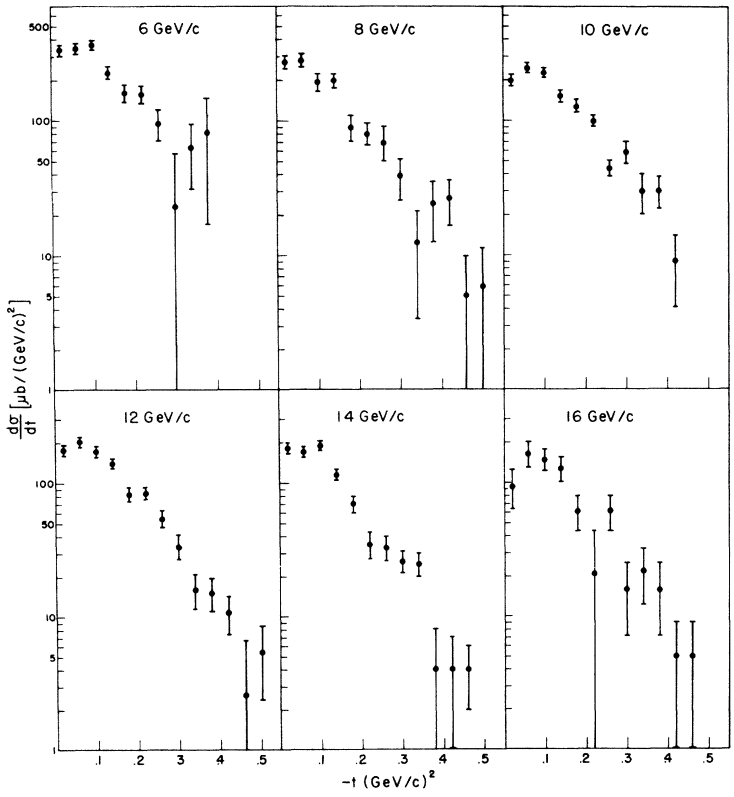

FIG. 2. The differential $\pi^- + p \to \pi^0 + n$ charge-exchange cross sections at 6, 8, 10, 12, 14, and 16 GeV/c. The errors shown are statistical only. The systematic uncertainties are ±8%.

The main features of the differential cross sections are the same at all incident momenta over the range of momentum transfer measured: $0 \geq t \geq -0.5$ (GeV/c)^2. The region between $t = 0$ and about $t = -0.1$ (GeV/c)^2 is rather flat, although there appears to be a slight dip near $t = 0$, which persists when the data are plotted in intervals with half the width of those used in Fig. 2. Beyond $t = -0.1$ (GeV/c)^2, there is an approximately exponential decrease, with slopes which closely approximate those observed in the elastic scattering of $\pi^- p$ and $\pi^+ p$.[7]

Using the fact that the differential cross section is flat within statistics out to about $t = -0.1$ (GeV/c)^2, the values of $(d\sigma/dt)_{t=0}$ are taken in each case as the average of the differential cross section between $t = 0$ and $t = -0.12$ (GeV/c)^2; if the differential cross section dips at $t = 0$, these estimates of $(d\sigma/dt)_{t=0}$ may be slightly high. As shown in Fig. 3(a), $(d\sigma/dt)_{t=0}$ goes down approximately as $1/p_{\pi^-}$. For all p_{π^-}, the value of $(d\sigma/dt)_{t=0}$ is well above that of the square of the imaginary part of the charge-exchange amplitude as calculated using the optical theorem, assuming charge independence, from the difference between the $\pi^- p$ and $\pi^+ p$ total cross sections.[8] This implies a nonzero difference between the real parts of the $\pi^- p$ and $\pi^+ p$ elastic-scattering amplitudes. These differences have been calculated and listed in Table I.

In this Table, column 1 is the incident-pion lab momentum. Column 2 is the difference, $\Delta\sigma$, between the $\pi^- p$ and $\pi^+ p$ total cross sections.[8] Column 3 shows the square of the imaginary part of the charge-exchange amplitude as calculated from $\Delta\sigma$. Column 4 contains our values of $(d\sigma/dt)_{t=0}$ for the charge-exchange cross section, including the systematic as well as statistical errors. Column 5 is the square of the real part of the charge-exchange amplitude, given by the difference between the values in columns 4 and 3. Column 6 gives the absolute value of the difference between the real parts of the $\pi^+ p$ and $\pi^- p$ elastic-scattering amplitudes at $t = 0$, given by the square root of two times the value listed in column 5.

Recently, Foley et al.[9] have obtained values for the real parts of the elastic-scattering amplitudes in the same energy region as this ex-

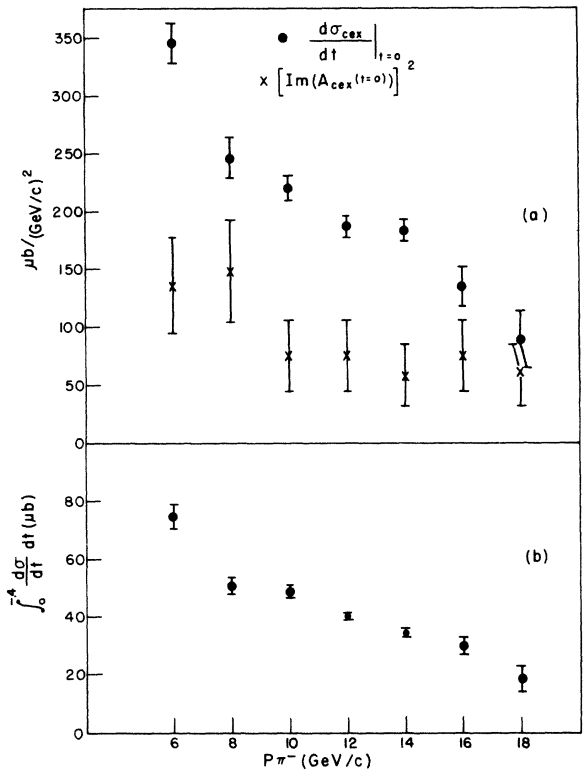

FIG. 3. (a) The differential charge-exchange cross section at $t = 0$ as a function of incident-pion lab momentum. As explained in the text, these values are obtained from the data in Fig. 2 by averaging the first three data points at each momentum. The errors shown are statistical only. For comparison, we have plotted the square of the imaginary part of the charge-exchange amplitude at $t = 0$, obtained from data in reference 8. (b) The values of the differential charge-exchange cross sections integrated between $t = 0$ and $t = -0.4$ (GeV/c)^2. If the differential cross sections, as shown in Fig. 2, continue to decrease exponentially for larger values of $-t$, these integrated values include about 95% of the total charge-exchange cross sections.

periment. Their measurements involved the interference of the real part with the Coulomb amplitude and made the assumption that the real and imaginary parts of the elastic-scattering amplitudes have the same t dependence over the interference region, about $t = 0.001$ to $t = 0.02$ (GeV/c)^2. If we take the difference between their real parts of the π^+p and π^-p elastic amplitudes, the value of this difference agrees, within their statistical errors, with our value in column 6 of Table I. However, inclusion of their systematic uncertainties produces an uncertainty in this difference which is at least as large as the difference itself, so that no meaningful quantitative comparison can be made.

Figure 3(a) and Table I show that, at all our energies, the real part of the $t = 0$ charge-exchange amplitude is of the same magnitude as the imaginary part. It is interesting to note that, on the basis of a $1/p_{\pi^-}$ dependence of $(d\sigma/dt)_{t=0}$, dispersion relations predict equality of the real and imaginary parts.

A detailed analysis[10] of these charge-exchange data in terms of the exchange of a single ρ trajectory shows that it is quite consistent with the predictions of the Regge-pole hypothesis. In particular, Regge theory and dispersion relations predict that $\mathrm{Re}(A_{cex})/\mathrm{Im}(A_{cex}) = \frac{1}{2}\tan\pi\alpha_\rho(t)$, where $\mathrm{Re}(A_{cex})$ and $\mathrm{Im}(A_{cex})$ are the real and imaginary parts of the charge-exchange amplitude, and $\alpha_\rho(t)$ is the trajectory of the ρ meson. The analysis of our data shows[10] that $\alpha_\rho(t = 0) \approx 0.6$, and is decreasing slowly and linearly for larger values of $-t$. This predicts that the values of $\mathrm{Re}(A_{cex})$ and $\mathrm{Im}(A_{cex})$ are approximately equal in the range of t from 0 to -0.1 (GeV/c)^2, and brings up an interesting point about the possible behavior of the real

Table I. The calculation of the absolute value of the difference between the real parts of the π^+p and π^-p elastic-scattering amplitudes at $t = 0$, using our data and the total π^+p and π^-p cross sections from reference 8.

p_{π^-} (GeV/c)	$\Delta\sigma$ (mb)	$[\mathrm{Im}(A_{cex}(t=0))]^2$ [μb/(GeV/c)^2]	$(d\sigma_{cex}/dt)_{t=0}$ [μb/(GeV/c)^2]	$[\mathrm{Re}(A_{cex}(t=0))]^2$ [μb/(GeV/c)^2]	$\lvert\mathrm{Re}(A_+)-\mathrm{Re}(A_-)\rvert$ [10^{-15} cm/(GeV/c)]
6	2.3 ± 0.36	135 ± 42	345 ± 45	210 ± 62	20.5 ± 3.0
8	2.4 ± 0.36	147 ± 44	246 ± 37	99 ± 57	14.1 ± 4.1
10	1.7 ± 0.36	74 ± 31	222 ± 29	148 ± 42	17.2 ± 2.4
12	1.7 ± 0.36	74 ± 31	186 ± 24	112 ± 39	15.0 ± 2.6
14	1.5 ± 0.36	57 ± 27	182 ± 24	125 ± 36	15.8 ± 2.3
16	1.7 ± 0.36	74 ± 31	134 ± 29	60 ± 42	11.0 ± 3.9
18	1.5 ± 0.36	57 ± 27	88 ± 34	31 ± 43	7.9 ± 5.5

parts of the $\pi^- p$ and $\pi^+ p$ elastic-scattering amplitudes:

The experimental evidence[11,12] indicates a possible equality, or near equality, of the $\pi^+ p$ and $\pi^- p$ differential cross sections near $t = -0.1$ $(\mathrm{GeV}/c)^2$. Assuming charge independence, $A_{\mathrm{cex}} = [A_+ - A_-]/\sqrt{2}$, where A_- and A_+ are the $\pi^- p$ and $\pi^+ p$ complex elastic-scattering amplitudes. Equality of these elastic-scattering differential cross sections to within a few times the value of the charge-exchange differential cross section, plus the approximate equality of $\mathrm{Re}(A_{\mathrm{cex}})$ and $\mathrm{Im}(A_{\mathrm{cex}})$ from the Regge interpretation of our data, would require that $\mathrm{Re}(A_+) \approx \mathrm{Im}(A_+)$ and $\mathrm{Re}(A_-) \approx \mathrm{Im}(A_-)$.

There is good experimental evidence[12] that at $t = 0$, $\mathrm{Re}(A_+)$ and $\mathrm{Re}(A_-)$ are quite a bit smaller than $\mathrm{Im}(A_+)$ and $\mathrm{Im}(A_-)$, respectively, independent of the assumption that the real and imaginary parts have identical t dependence. This would indicate that the ratios $\mathrm{Re}(A_+)/\mathrm{Im}(A_+)$ and $\mathrm{Re}(A_-)/\mathrm{Im}(A_-)$ are increasing from about 0.2 or 0.3 at $t = 0$ to about 1.0 at $t = -0.1$ $(\mathrm{GeV}/c)^2$, requiring that the real parts of the elastic amplitudes have a different t dependence than the imaginary parts. It must be emphasized that this conclusion requires the following conditions: equality, within the limits mentioned above, of the elastic $\pi^+ p$ and $\pi^- p$ differential cross sections at a fairly low value of $-t$, correctness of the Regge-theory interpretation of the charge-exchange scattering in terms of the exchange of a single ρ trajectory, and also charge independence and dispersion relations.

In Fig. 3(b) are shown the values of the differential charge-exchange cross sections integrated between $t = 0$ and $t = -0.4$ $(\mathrm{GeV}/c)^2$. These integrated values include about 95% of the total charge-exchange cross sections if the differential cross sections, as shown in Fig. 2, continue to decrease exponentially for larger values of $-t$.

We would like to acknowledge the hospitality and assistance of the Brookhaven National Laboratory and its staff during the experimental run at the A.G.S. O. Fackler, E. Shibata, C. Ward, S. Smith, P. Kirk, and T. Kan assisted during the running of this experiment, and F. Sergiampietri and R. Casali helped with the data analysis. All computer calculations have been carried out at the Centro Calcoli del Comitato Nazionale per l'Energia Nucleare and Centro Nazionale Analisi Fotogrammi, Bologna, Italy We thank T. Lyons and C. Strumski for their help with experimental equipment, and the scanning group at Pisa for their diligence. We are especially indebted to L. Stinson for his assistance, and to Professor D. Frisch for his advice and support throughout the experiment.

---

*This work is supported in part through funds provided by the U. S. Atomic Energy Commission. The experiment itself was carried out at the Alternating Gradient Synchrotron at Brookhaven National Laboratory, supported by the U. S. Atomic Energy Commission.

†This author wishes to thank the Brookhaven National Laboratory for their support as a Research Collaborator during part of the running of this experiment.

‡Present address: American Science and Engineering, Inc., Cambridge, Massachusetts.

[1]As far as we know these are the first extensive $\pi^- p$ charge-exchange measurements above 6 GeV/c. Previously, upper limits have been obtained at 6 and 18 GeV/c [G. Bellini, E. Fiorini, and A. Orkin-Lecourtois, Phys. Letters 4, 164 (1963)] and a $\pi^+ n$ charge-exchange measurement has been made at 6 GeV/c [F. Bruyant, M. Goldberg, G. Vegni, H. Winzeler, P. Fleury, J. Huc, R. Lestienne, G. DeRosny, and R. Vanderhaghen, Phys. Letters 12, 278 (1964)]. Also, preliminary results of this experiment and that of the Falk-Vairant group in this same energy region have been presented in Proceedings of the International Conference on High Energy Physics, Dubna, 1964 (to be published).

[2]M. A. Wahlig, I. Mannelli, L. Sodickson, O. Fackler, C. Ward, T. Kan, and E. Shibata, Phys. Rev. Letters 13, 103 (1964).

[3]W. Galbraith, E. W. Jenkins, T. F. Kycia, B. A. Leontić, R. H. Phillips, A. L. Read, and R. Rubinstein, Proceedings of the International Conference on High Energy Physics, Dubna, 1964 (to be published).

[4]We would like to thank W. Galbraith, E. W. Jenkins, and T. F. Kycia for information on the characteristics of this beam and the use of their Cherenkov counter.

[5]S. J. Lindenbaum and R. M. Sternheimer, Phys. Rev. 105, 1874 (1957).

[6]M. Deutschmann, R. Schulte, H. Weber, W. Woischnig, C. Grote, J. Klugow, S. Nowak, S. Brandt, V. T. Cocconi, O. Czyzewski, P. F. Dalpiaz, G. Kellner, and D. R. O. Morrison, Phys. Letters 12, 356 (1964).

[7]S. J. Lindenbaum, Proceedings of the International Conference on Nucleon Structure at Stanford University, 1963, edited by R. Hofstadter and L. I. Schiff (Stanford University Press, Stanford, California, 1964), p. 105.

[8]W. Galbraith, E. W. Jenkins, T. F. Kycia, B. A. Leontić, R. H. Phillips, A. L. Read, and R. Rubinstein (to be published).

[9]K. J. Foley, R. S. Jones, R. S. Gilmore, S. J. Lindenbaum, W. A. Love, S. Ozaki, E. H. Willen, R. Yamada, and L. C. L. Yuan, Proceedings of the Interna-

tional Conference on High Energy Physics, Dubna, 1964 (to be published).

[10]R. K. Logan, following Letter [Phys. Rev. Letters 14, 414 (1965).

[11]K. J. Foley, S. J. Lindenbaum, W. A. Love, S. Ozaki, J. J. Russell, and L. C. L. Yuan, Phys. Rev. Letters 10, 543 (1963).

[12]K. J. Foley, S. J. Lindenbaum, W. A. Love, S. Ozaki, J. J. Russell, and L. C. L. Yuan, Phys. Rev. Letters 11, 425 (1963).

[13]J. D. Jackson and H. Pilkuhn, Nuovo Cimento 33, 906 (1964); N. Armenise, B. Ghidini, S. Mongelli, A. Romano, P. Waloschek, J. Laberrigue-Frolow, Nguyen Huu Khanh, C. Ouannes, M. Sené, and L. Vigneron, Phys. Letters 13, 341 (1964), and references quoted there.

SINGLE REGGE-POLE ANALYSIS OF $\pi^- p$ CHARGE-EXCHANGE SCATTERING*

Robert K. Logan
Laboratory for Nuclear Science and Physics Department,
Massachusetts Institute of Technology, Cambridge, Massachusetts
(Received 25 January 1965)

The measurement of the $\pi^- p$ charge-exchange differential cross section described in the preceding Letter by Mannelli et al.[1] provides an excellent test of the Regge-pole hypothesis. The particle or resonance exchanged in the crossed channel must have isotopic spin ≥ 1, zero baryon number, positive G parity, and parity $(-1)^J$, where J is the spin of the particle. The only presently known candidate is the ρ meson. However, if the presently accepted spin and parity assignments for the B meson are not correct, the B could conceivably be exchanged as well.

We assume in our analysis that only the ρ trajectory is exchanged. Our expression for the differential cross section, including both the spin-flip and spin-nonflip contributions, is thus given by[2]

$$\frac{d\sigma_{\text{cex}}}{dt}=\frac{B^2(t)}{16\pi}\left|\frac{1-e^{-i\pi\alpha(t)}}{\sin\pi\alpha(t)}\right|^2\left(\frac{s}{2m_\pi m_N}\right)^{2\alpha(t)-2}, \quad (1)$$

where m_π and m_N are the pion and nucleon masses, $\alpha(t)$ is the trajectory of the ρ, s and t are the usual Mandelstam variables, and

$$B^2(t)=|b^{(1)}(t)|^2-\frac{t}{4m_N^2}|b^{(1)}(t)-\alpha(t)b^{(2)}(t)|^2.$$

The first term in the expression for $B^2(t)$ is the spin-nonflip contribution whereas the second arises from pure spin flip. From this it follows that $b^{(1)}$ and $b^{(2)}$ are related to the ρ coupling constants as follows:

$$b^{(1)}(m_\rho^2)=2\pi\epsilon\gamma_{\rho\pi\pi}\gamma_{\rho NN}$$

$$b^{(1)}(m_\rho^2)-\alpha(m_\rho^2)b^{(2)}(m_\rho^2)=4\pi\epsilon\gamma_{\rho\pi\pi}m_N\mu_{\rho NN}, \quad (2)$$

where

$$\epsilon=\mathrm{Re}\frac{d\alpha(t)}{dt}\Big|_{t=m_\rho^2}.$$

Making use of the high-energy approximation $s\approx 2m_N E$, where E equals the total energy of the incident pion in the laboratory system and simplifying our expression for $d\sigma_{\text{cex}}/dt$, we obtain

$$\frac{d\sigma_{\text{cex}}}{dt}=\frac{B^2(t)}{16\pi}\{1+\tan^2[\tfrac{1}{2}\pi\alpha(t)]\}\left(\frac{E}{m_\pi}\right)^{2\alpha(t)-2}. \quad (3)$$

This equation predicts that a plot of $\ln(d\sigma/dt)$ versus $\ln E$ at constant t will yield a straight line with slope $2\alpha(t)-2$. In order to verify the above prediction and to determine the slope we performed a least-squares fit of $\ln(d\sigma/dt)(E,t)$ to the form

$$\sum_{n=0}^{N} m_n(t)(\ln E)^n$$

at constant t using the data of Mannelli et al.[1] at $P_{\text{lab}}=6$, 8, 10, 12, 14, and 16 GeV/c. We used t intervals of 0.04 (GeV/c)^2 from $t=0$ to $t=-0.32$ (GeV/c)^2. For all values of t, reasonable straight-line fits to the data were obtained (see Fig. 1). At certain values of t we obtained slightly better fits for $N=2$ and 3. We can exclude these fits, however, since their extrapolation to 3.8 GeV/c gives results which are in contradiction with existing experimental data.[3]

From $m_1(t)$, the slope of the straight-line fit, we obtain the trajectory $\alpha(t)$ which is listed in Table I. Fitting these values of $\alpha(t)$, with the constraint that $\alpha(t=m_\rho^2)=1$, to polynomials